



## Application of soybean residue (okara) as a low-cost adsorbent for reactive dye removal from aqueous solution

Jingfeng Gao\*, Chunying Si, Yang He

*College of Environmental and Energy Engineering, Beijing University of Technology, 100 Pingleyuan, Chaoyang District, Beijing 100124, China*

*Tel. +86 10 67391918; Fax: +86 10 67391983; email: gao158@gmail.com*

Received 20 September 2013; Accepted 30 October 2013

### ABSTRACT

This study investigated the feasibility of using okara as a low-cost adsorbent for the removal of Reactive Brilliant Blue KN-R (RBB), a typical reactive dye, from aqueous solution. Batch adsorption experiments were conducted to evaluate the effects of pH, adsorbent dosage, initial dye concentration, and temperature. It was proved that strong acidic condition was favorable for the adsorption process and the optimal pH was 2.0. Langmuir–Freundlich (L–F) isotherm fitted well with the equilibrium data. The maximum adsorption capacity determined from the L–F isotherm was 68.67, 159.60, and 402.58 mg/g at 20, 35, and 50°C, respectively. Kinetic studies showed that adsorption of RBB followed the pseudo-second-order kinetic model, both boundary layer diffusion and intra-particle diffusion might affect the adsorption rate. Thermodynamic study demonstrated the spontaneous and endothermic natures of the adsorption process. Fourier transform infrared analysis revealed that chemical functional groups (e.g. amine, hydroxyl, carboxyl, phosphate, and ether) on okara would be the active binding sites for adsorption of RBB. The results showed that okara could be effectively used as a low-cost and alternative adsorbent for the removal of RBB from wastewater.

*Keywords:* Okara; Adsorption; Reactive Brilliant Blue KN-R; Isotherm; Kinetic

### 1. Introduction

Synthetic dyes are extensively used in textile, tannery, paper and pulp, plastic, and many other industries. It is reported that there are over 100,000 commercial dyes with a rough estimated production of  $7 \times 10^5$ – $1 \times 10^6$  tons per year worldwide [1]. Approximately 10–20% of the dyes are released into the environment during manufacturing and usage [2]. A large

fraction, usually around 30% of the applied reactive dyes, is wasted because of dye hydrolysis in the alkaline dye-bath [3]. Moreover, the presence of very small amounts of dyes in water is highly visible and even results in bad smell. Thus, the effluents of hazardous dyes have created a global concern. The treatment of dyes wastewater is not easy due to dyes' complex structure, toxicity, high thermal, and photo-stability. Hence, removal of dyes from wastewater is desirable and the development of clean-up technologies for the treatment of water contaminated with dyes is of major interest [4].

\*Corresponding author.

Various technologies have been employed for the removal of dyes from wastewaters. The concentrated residue left after membrane filtration poses disposal problems, and high capital cost, possibility of clogging, and membrane replacements are its disadvantages [5]. Coagulation technique requires significant quantities of chemicals and produces large amounts of sludge [6]. Advanced oxidation processes (such as UV/oxidant, Fenton, Ozonation [7]) can be quite effective for dye removal, but high cost and intensive energy requirements limit their application. The biological treatment may result in the generation of colorless dead end aromatic amines, which are generally more toxic than the parent compounds [8]. Among all the available physical, chemical, or biological methods of dyes containing wastewater treatment, adsorption is regarded as one of the most potential technologies due to its high efficiency and ability to separate wide range of chemical compounds. Much interest has been focused on activated carbon as an effective adsorbent to remove various dyes. However, the high unit cost of the activated carbon (about 1 US dollar/kg) and the absence of reliable methods for adsorbent regeneration (thermal regeneration costs are about 1–2 US dollar/kg) restrict its application [9]. Thus, adsorption by some low-cost adsorbent has gained considerable attention in the recent years. A large variety of non-conventional materials have been investigated as adsorbents, such as bottom ash [10–12], de-oiled soya [11,13,14], hen feather [15–18], coconut-husk [19], wheat husk [20], and eggshell waste [21–23]. Meanwhile, food waste raise interest of scientists, because every year almost 45 billion kg of fresh vegetables, fruits, milk, and grain products are lost to waste in the USA and in the UK, 20 million tons of food waste are produced annually [24].

Our study is another attempt to explore the possibility and feasibility of utilizing okara, the residue left from ground soy beans produced soy milk and *tofu*, as economic and effective adsorbent for the removal of dyes from wastewaters. About 1.1 kg of fresh okara is produced from every kilogram of soybeans processed for soymilk production [25]. In China, about 2,800,000 tons of okara are produced annually [26]. Large quantities of okara produced annually pose a significant disposal problem due to its tendency to deteriorate very quickly. Lots of studies have been undertaken to develop uses of okara, some of which has been directed to dietary additive in biscuits and snacks, but its use as a human food is constrained by its high fiber content [25]. In addition, okara contains mostly crude fiber composed of cellulose, hemicellulose, and lignin [25], which might be useful for decolorizing dyes through different mechanisms.

Based on the principle of waste control by waste, the present work is an attempt to use okara as adsorbent to remove dyes from wastewater. Utilizing okara as a low-cost and alternative adsorbent will increase economic value of okara and reduce the cost of waste disposal, and besides this, dye pollution reduction can be achieved.

Of the dyes, reactive dyes are unique textile colorants because they contain reactive groups that bind to fibers through formation of covalent bonds. Approximately, 40 types of reactive groups have been listed for the commercial dyes and the highest volume commercial products are those containing the 2-sulfatoethyl sulfone moiety [27]. Reactive Brilliant Blue KN-R (RBB, C.I. Reactive Blue 19), which is a representative of this type of reactive dye. As a typical anthraquinone dye, RBB has good chromaticity and is widely used for dyeing cotton fabric and other cellulose [28]. For the majority of vinyl sulfone reactive dyes, the degree of fixation ranges from 75 to 80% on cotton, which means that 20–25% of the dyes enter the waste stream. Generally, the toxicity and inhibition of RBB in microorganisms cause difficulty in biodegrading the dyes. For example, it was verified that less than 100 mg/L of RBB was enough to completely inhibit the methane production of both mesophilic and thermophilic inocula [29]. Also, the results of a *saccharomyces cerevisiae* test illustrated that the toxicity, teratogenicity, and carcinogenicity increased with RBB concentration increasing from 5 to 125 mg/L [30]. Thus, RBB was selected as model compound in this study.

The main objective of the study is to examine the feasibility of using okara as economic, effective, and novel adsorbent to remove RBB from aqueous solution. The effects of different parameters, such as pH value, adsorbent dosage, initial dye concentration, and temperature were studied to optimize the adsorption process. Three isotherms, namely Langmuir, Freundlich, and Langmuir–Freundlich (L–F) isotherm, were used to analyze the adsorption equilibrium data. Pseudo-first-order, pseudo-second-order, and intraparticle diffusion models were applied to describe the adsorption process of RBB onto okara. Thermodynamics parameters were calculated using the equilibrium data obtained at different temperatures. Furthermore, the Fourier transform infrared (FTIR) analysis was carried out to elucidate the interaction mechanisms.

## 2. Materials and methods

### 2.1. Preparation and characterization of adsorbent

The fresh okara was kindly provided by a local soybean milk factory in Beijing. It was first sieved to

the desired mesh size (0.5–0.8 mm), and then freeze-dried using Labconco FreeZone 1L (Labconco, America) to yield adsorbent. The resulting dried okara was stored in desiccators ready for use. The surface morphology of okara was qualitatively analyzed by scanning electronic microscopy (SEM) (Hitachi S-4300, Japan). The textural properties of okara were measured by N<sub>2</sub> adsorption at 77 K in an ASAP 2020 apparatus (Micromeritics, USA).

Additionally, in order to characterize the surface functional groups presented on the adsorbent surface, the okara before and after adsorption was analyzed by FTIR using a Bruker Vertex 70 FTIR spectrometer, which may reveal the possible dye decolorization mechanisms. The okara was first freeze-dried using Labconco FreeZone 1L, then they were mixed with KBr in the ratio of 1:100 and compacted to pellet form under high pressure. The pellet was immediately analyzed in the range of 400–4,000 cm<sup>-1</sup> with a resolution of 4 cm<sup>-1</sup>.

## 2.2. Dyes and analysis

RBB (molecular formula = C<sub>22</sub>H<sub>16</sub>N<sub>2</sub>Na<sub>2</sub>O<sub>11</sub>S<sub>2</sub>, λ<sub>max</sub> = 595 nm) was purchased from Tianjin Shengda Chemical Factory (China). Its chemical structure is shown in Fig. 1. The test dye solutions were prepared by diluting stock solutions to the desired concentrations. Prior to adding okara to the dye solution, the pH of each solution was adjusted to the required value with 0.1 mol/L HCl or NaOH solutions with a pH-meter (WTW 340i, Germany) for the measurements.

Samples were taken at given time intervals and residual RBB concentration was determined using a UV–vis spectrophotometer (UV-2802PC, Unico, Shanghai, China) at 595 nm. The equilibrium adsorption capacity of RBB was calculated using Eq. (1):

$$q_e = \frac{V(C_0 - C_e)}{m} \quad (1)$$

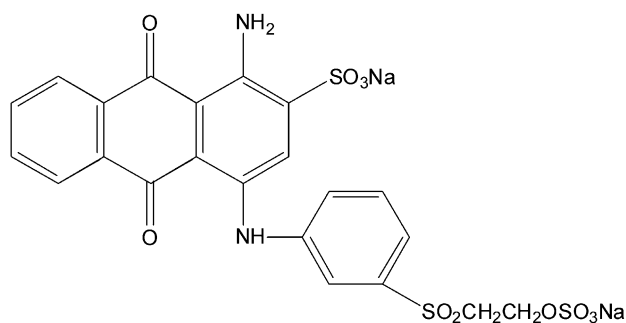


Fig. 1. Chemical structure of RBB.

where  $C_0$  and  $C_e$  is the initial and equilibrium dye concentration in the solution (mg/L);  $V$  is the volume of the dye solution (L); and  $m$  is the weight of adsorbent used (g). The decolorization efficiency can be calculated by Eq. (2):

$$\text{Decolorization efficiency} = \frac{C_0 - C_e}{C_0} \times 100\% \quad (2)$$

## 2.3. Batch adsorption experiments

Batch experiments were conducted in 50 mL Erlenmeyer flasks, which were agitated in a water bath shaker (GFL 1086, Germany) with a shaking rate of 150 rpm at a constant temperature of 20 ± 1 °C (except for isotherms experiments) until reaching equilibrium. Each test was monitored for 24 h. Adsorption of RBB on the walls of the flasks was found negligible by running the control experiments.

To investigate the effect of initial solution pH value on the adsorption capacity, the initial pH value varied in the range of 2.0–11.0, with the okara concentration fixed at 10 g/L and the initial RBB concentration of 50 mg/L. The optimal pH value was used for the subsequent experiments. To study the effect of adsorbent dosage, adsorbent concentration was varying from 4 to 20 g/L, initial RBB concentration was fixed at 60 mg/L, and adsorbent dosage of 4 g/L was selected for the following experiments. To investigate the effect of initial dye concentration on adsorption, initial RBB concentration ranged from 40 to 200 mg/L. The equilibrium, kinetics, and thermodynamic experiments were performed at temperatures in the range of 20–50 °C, and initial RBB concentration was in the range of 40–200 mg/L.

## 3. Results and discussion

### 3.1. Characterization of the adsorbent

#### 3.1.1. SEM and BET analysis

The morphology of okara was ascertained with the help of SEM photographs (Fig. 2). Fig. 2 exhibited its inhomogeneity, parts of okara were dried persimmon-like (Fig. 2(a)), and parts were rod-like with lots of large pores on it (Fig. 2(b)). The large pores enabled a deeper penetration of RBB molecules to the internal pore structure of okara, and increased the possibility of RBB molecules to be contacted and adsorbed onto okara. The total pore volume and average pore diameter were found to be 0.000875 cm<sup>3</sup>/g and 4.29 nm. The BET surface area of okara was found to be 8,155 cm<sup>2</sup>/g, which was larger than the surface area (728.6 cm<sup>2</sup>/g) of de-oiled Soya [31], a kind of waste biomaterial having been used in treating dye wastewater.

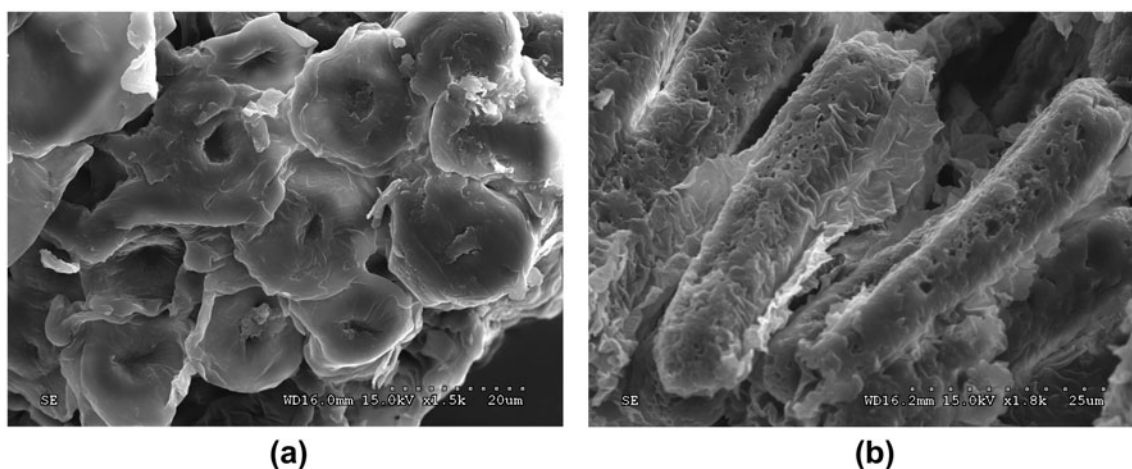


Fig. 2. SEM photographs of okara.

### 3.1.2. FTIR analysis

The FTIR spectra of okara before and after adsorption are shown in Fig. 3. The FTIR spectra of okara before adsorption (Fig. 3(a)) displayed a number of absorption peaks, reflecting the complex properties of okara. The band at  $3,436\text{ cm}^{-1}$  might be due to the overlapping of stretching vibration of O–H and N–H of hydroxyl and amine groups. The band at  $2,926$  and  $2,855\text{ cm}^{-1}$  represented an asymmetric vibration of  $\text{CH}_2$  and stretching vibration of the C–H group, respectively. The band observed at  $1,745\text{ cm}^{-1}$  could be due to a C=O group of carboxylic acid or its ester. The band at  $1,641\text{ cm}^{-1}$  might indicate the presence of carboxyl, and C=N, N–H, and C=O groups of amide I. While a  $1,547\text{ cm}^{-1}$  band could be due to deformation vibration of N–H (amide II) peptide bond of protein. Band located at  $1,457\text{ cm}^{-1}$  might represent the asymmetric C–H deformations. The band at  $1,238\text{ cm}^{-1}$

implied the N–H bending vibrations of peptide amide III. The band at  $1,092\text{ cm}^{-1}$  could be assigned to the phosphate group and C–O group of polysaccharide.

Fig. 3(b) shows the changes in the FTIR spectra of okara after adsorption. There were significant similarities in the spectra before and after adsorption, suggesting that the components and structure of okara remained intact. After adsorption, the band at  $3,436\text{ cm}^{-1}$  did not shift and the band intensity decreased sharply. One reason may be the breaking of hydrogen bonds of hydroxyl (O–H) and amine (N–H) groups. However, the hydroxyl groups of okara are incapable of forming hydrogen bonds with RBB dyes. And electrostatic interaction between amine ( $\text{R-NH}_3^+$ ) of okara and  $\text{SO}_3^-$  of RBB may not lead to the breaking of hydrogen bonds. So the breaking of hydrogen bonds may not be the reason, other chemical or physical interactions may be involved. The band intensity of

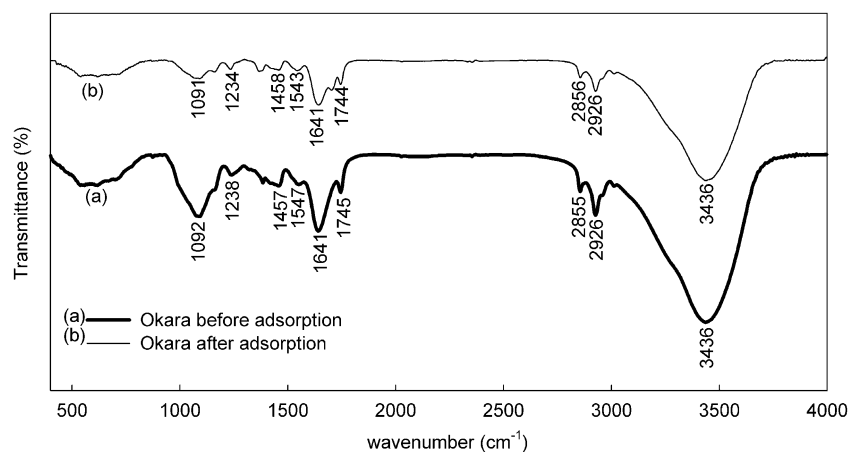


Fig. 3. FTIR spectra of okara before and after RBB adsorption. (a) Before RBB adsorption; (b) after RBB adsorption.

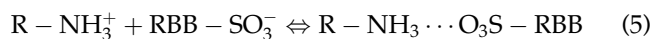
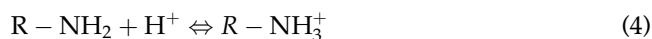
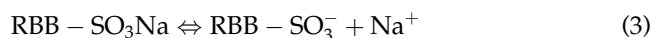
2,926  $\text{cm}^{-1}$  decreased and the band did not shift. The reason may be that some of the RBB molecules were adsorbed by forming a hydrophobic interaction between the  $\text{CH}_2$  of okara and the hydrophobic part of RBB. After adsorption, the band at 1,547 and 1,238  $\text{cm}^{-1}$  shifted to lower frequency of 1,543 and 1,234  $\text{cm}^{-1}$ , respectively, and the band intensity decreased, indicating the electrostatic attraction between  $\text{SO}_3^-$  of RBB and amide II and amide III groups ( $\text{R-NH}_3^+$ ) of okara may be one reason for the bands shift. Comparing with the band at 1,547 and 1,238  $\text{cm}^{-1}$ , the band at 1,641  $\text{cm}^{-1}$  did not shift, suggesting that C=N, N-H, and C=O groups of amide I might play a minor role in the adsorption than amide II and amide III groups. The band at 2,855 and 1,457  $\text{cm}^{-1}$  shifted to higher frequency of 2,856 and 1,458  $\text{cm}^{-1}$ , respectively, and band intensity decreased sharply, suggesting C-H group on okara took part in the adsorption. The band at 1,745 and 1,092  $\text{cm}^{-1}$  shifted to lower frequency of 1,744 and 1,091  $\text{cm}^{-1}$  and band intensity decreased, indicating that there would be reactions of RBB with phosphate group, C-O group of polysaccharide, and C=O group of carboxylic acid. As seen from the FTIR analysis, the complexity of the okara made the adsorption process much more complicated, and there can be several types of interactions: (1) electrostatic interaction between the electron-rich sites on the okara and the dye molecules, especially the interaction between  $\text{SO}_3^-$  of the RBB dye and the amine ( $\text{R-NH}_3^+$ ) groups of okara; (2) physical interaction, such as hydrogen bonding, hydrophobic attractions, and (3) chemical interaction between okara component and RBB dye molecules. These interactions can happen simultaneously. FTIR results demonstrated the main functional groups for adsorption of RBB onto okara would be amine, hydroxyl, carboxyl, phosphate, and ether. However, the FTIR spectrum changes only gave the possible involvement of those functional groups on okara, more investigations are needed to elucidate the adsorption mechanism.

### 3.2. The factors influencing RBB adsorption onto okara

#### 3.2.1. Effect of initial solution pH value

Fig. 4 shows the relationship between the dye adsorption capacity and the pH value at  $20 \pm 1^\circ\text{C}$ . It could be seen from Fig. 4 that the equilibrium adsorption capacity decreased dramatically with the pH value increasing from 2.0 to 6.0 and a plateau was observed with pH higher than 6.0. The maximum uptake of RBB was obtained at pH value of 2.0. Hence, an optimum pH value of 2.0 was selected for further investigations. The influence of pH on RBB

adsorption could be demonstrated on the basis of the ionic interactions. The hydrolysis constant of the sulfonate ( $\text{SO}_3^-$ ) groups on the anionic dye RBB is 2.1 [32], meaning that the functional group could be easily dissociated. Thus, the dye molecule has net negative charges in the acid solution. Some important functional groups, like amine ( $-\text{NH}_2$ ) groups, will be positively charged ( $-\text{NH}_3^+$ ) in acid solution for the presence of  $\text{H}^+$ . At lower pH, more protons will be available to protonate amino groups of okara to form groups  $-\text{NH}_3^+$ . In this case, higher uptakes of dye obtained at lower pH values may be in terms of the electrostatic attractions between the negatively charged dye's anions and positively charged surface of okara. The mechanisms of RBB adsorption onto okara could be displayed in Eqs. (3)–(5).



A lower adsorption at higher pH values may be due to the presence of  $\text{OH}^-$  ions competing with the dye anions for the adsorption sites, also because of ionic repulsion between the negatively charged binding sites of okara and the anionic dye molecules. Similar results were reported for the adsorption of RBB from aqueous solutions on modified bentonite [33].

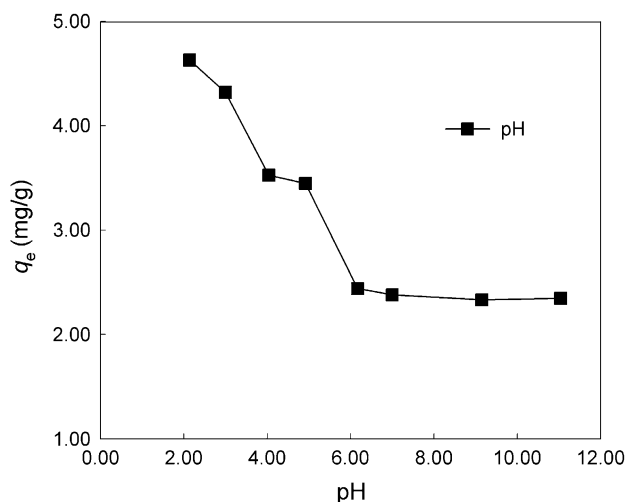


Fig. 4. Effect of initial solution pH value ( $C_0 = 50 \text{ mg/L}$ , adsorbent dosage = 10 g/L, temperature =  $20 \pm 1^\circ\text{C}$ ) on the adsorption of RBB by okara.

### 3.2.2. Effect of adsorbent dosage

Fig. 5 shows the amount of dye removed as a function of adsorbent dosage at 60 mg/L of initial dye concentration. The Fig. 5 clearly indicates that decolorization efficiency increased with increasing adsorbent dosage. When okara dosage was 20 g/L, decolorization efficiency was 95.38%. This might be due to an increase in the number of active sites of the adsorbent and availability of more adsorption sites with increasing amount of adsorbent. However, the equilibrium adsorption capacity  $q_e$  decreased from 13.05 to 2.73 mg/g with adsorbent dosage increasing from 4 to 20 g/L. Such a trend might be mainly due to aggregation or overlapping of adsorption sites, resulting in a decrease in total adsorbent surface area available to the dye and an increase in diffusion path length [1]. Based on an overall consideration of decolorization efficiency and equilibrium adsorption capacity, okara concentration of 4 g/L was selected as the optimal dosage and used for the subsequent experiments.

### 3.2.3. Effect of initial dye concentration

Fig. 6 reveals the dye amounts adsorbed per unit mass of adsorbent versus contact time at different initial RBB concentrations in the range of 40–200 mg/L. According to Fig. 6, it was evident that an important part of RBB was removed in the initial 45 min for all of the initial concentrations studied and then the speed of adsorption decreased gradually until reaching the equilibrium. In the initial stage, the adsorption sites on okara were bare and so adsorption rate was high. With adsorption going on, the amount

of adsorption sites available on the okara decreased, resulting in the decrease of adsorption rate. In addition, the  $q_e$  increased from 9.28 to 48.60 mg/g with initial dye concentration increasing from 40 to 200 mg/L. This indicated that increasing in dye concentration decreased the resistance toward dye uptake and increased the mass driving force among adsorbent and adsorbate, which increased the adsorption capacity [4].

### 3.3. Adsorption isotherm

To optimize the design of an adsorption system, it is necessary to establish the appropriate correlation for the equilibrium curves. The adsorption isotherm is the most important information which indicates how the adsorbate molecules distribute between the solid phase and the liquid phase as the adsorption process reaches the equilibrium state. Various isotherm models like Langmuir [34], Freundlich [35], and L-F [4] were used to describe the equilibrium adsorption in this work.

#### 3.3.1. Langmuir isotherm

The Langmuir adsorption model assumes that uptake of adsorbate occurs on a homogeneous surface by monolayer adsorption without any interaction between the adsorbed ions [34]. It also considers that there is no transmigration of the adsorbate in the plane of the surface of the adsorbent. The mathematical form of the Langmuir equation can be expressed as Eq. (6):

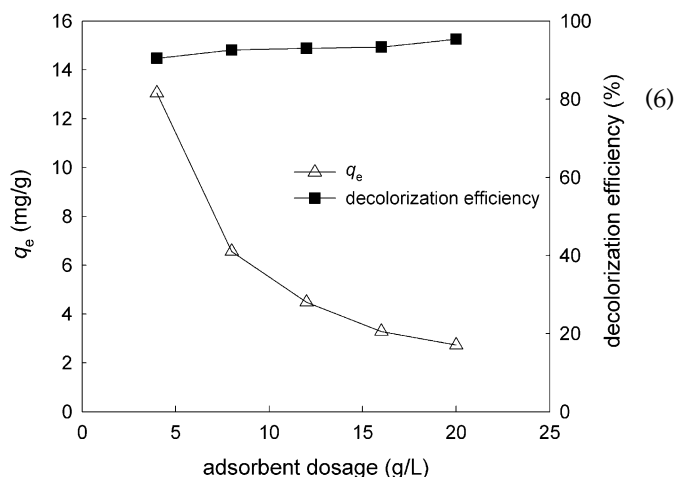


Fig. 5. Effect of adsorbent dosage ( $C_0 = 60$  mg/L, initial pH value  $2.0 \pm 0.1$ , temperature =  $20 \pm 1$  °C) on the adsorption of RBB by okara.

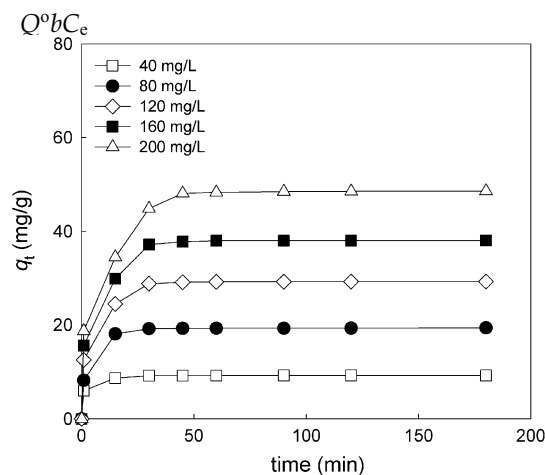


Fig. 6. Effect of initial dye concentration (adsorbent dosage = 4 g/L, initial pH value  $2.0 \pm 0.1$ , temperature =  $20 \pm 1$  °C) on the adsorption of RBB by okara.

where  $Q^0$  denotes the maximum adsorption capacity (mg/g) and  $b$  is Langmuir constant related with the energy of the adsorption (L/mg). The linear form of Langmuir isotherm can be written as Eq. (7):

$$\frac{C_e}{q_e} = \frac{C_e}{Q^0} + \frac{1}{bQ^0} \quad (7)$$

Fig. 7(a) shows the linearized Langmuir isotherm of RBB on okara obtained at  $20 \pm 1$ ,  $35 \pm 1$ , and  $50 \pm 1$  °C. A plot of  $C_e/q_e$  versus  $C_e$  yielded a straight line with slope  $1/Q^0$  and intercept  $1/Q^0b$ . Table 1 lists the computed values of  $Q^0$ ,  $b$ , and  $R^2$  at different temperatures. As seen from Fig. 7(a) and Table 1, the values of the correlation coefficients  $R^2$  were in the range of 0.0144–0.7932, and the maximum adsorption capacity  $Q^0$  and constant  $b$  were negative, so Langmuir isotherm did not fit the equilibrium data.

### 3.3.2. Freundlich isotherm

Fig. 7(b) shows the linearized Freundlich isotherms of RBB on okara obtained at  $20 \pm 1$ ,  $35 \pm 1$ , and  $50 \pm 1$  °C. The Freundlich isotherm is an empirical equation based on a heterogeneous surface and the empirical equation is expressed by the following Eq. (8):

$$q_e = K_F C_e^{1/n} \quad (8)$$

The linear form of Freundlich adsorption model is given by following Eq. (9):

$$\ln q_e = \ln K_F + \frac{1}{n} \ln C_e \quad (9)$$

$K_F$  represents the quantity of dye adsorbed onto adsorbent for an equilibrium concentration, (mg/g)  $(L/mg)^{1/n}$ . The slope  $1/n$ , which ranges between 0 and 1, is a measure of surface heterogeneity or adsorption intensity, becoming more heterogeneous as its value gets closer to zero [35]. The values of  $K_F$  and  $n$  obtained from the intercept and the slope of the plot of  $\ln q_e$  versus  $\ln C_e$  are also given in Table 1 along with the correlation coefficients. Although the correlation coefficients  $R^2$  ranged from 0.9390 to 0.9866, the values of  $1/n$  were greater than unity at 20 and 35 °C. Thus, it was not appropriate to describe the adsorption process of RBB onto okara by a heterogeneous surface isotherm model.

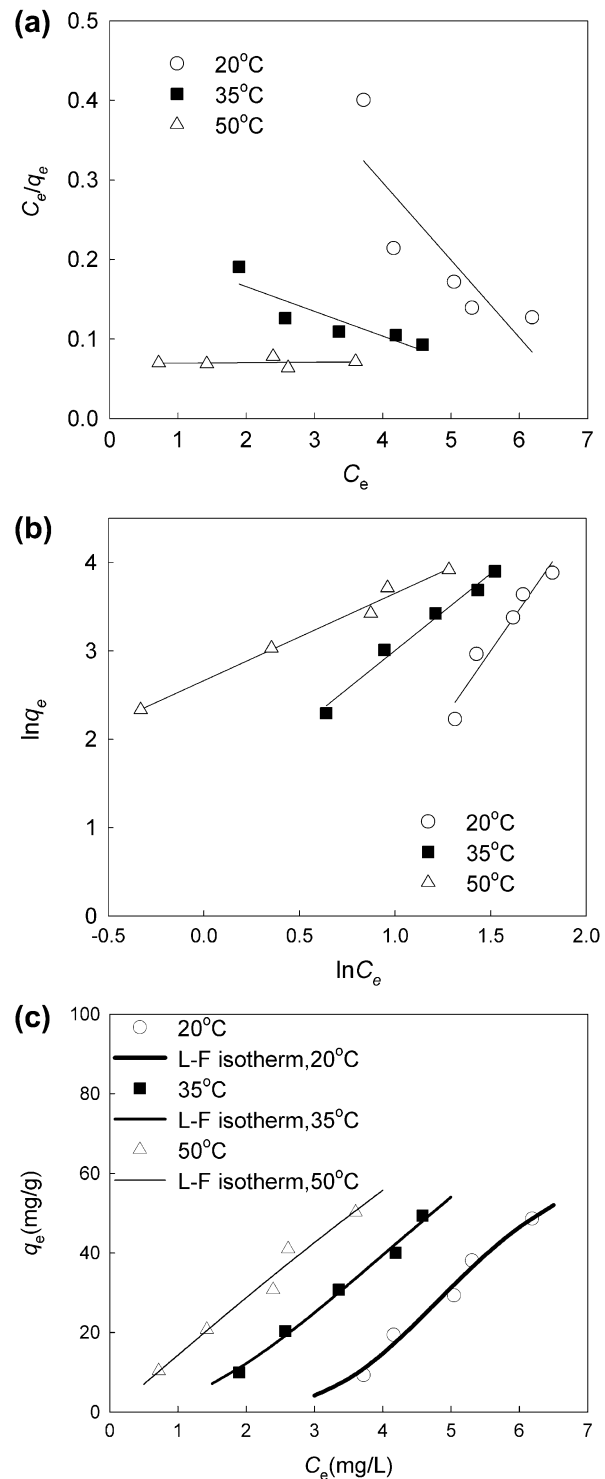


Fig. 7. Adsorption isotherms for RBB adsorption by okara at different temperatures. (a) Langmuir isotherm; (b) Freundlich isotherm; (c) L-F isotherm ( $C_0 = 40, 80, 120, 160$  and  $200$  mg/L, adsorbent dosage =  $4$  g/L, initial pH value  $2.0 \pm 0.1$ , temperature =  $20 \pm 1, 35 \pm 1$ , and  $50 \pm 1$  °C).

Table 1  
Isotherm constants for the adsorption of RBB on okara at various temperatures

Temperature (°C)	20	35	50
Langmuir isotherm			
$Q^0$ (mg/g)	–10.27	–32.15	1666.67
$b$ (L/mg)	–0.1420	–0.1365	0.0087
$R^2$	0.7244	0.7932	0.0144
Freundlich isotherm			
$K_F$ (mg/g)(L/mg) <sup>1/n</sup>	0.19	3.55	14.34
$n$	0.3196	0.5758	1.0121
$R^2$	0.9390	0.9843	0.9866
L–F isotherm			
$Q^0$ (mg/g)	68.67	159.60	402.58
$b$ (L/mg)	0.0003	0.0209	0.0368
$n$	0.1990	0.5034	0.9405
$R^2$	0.9811	0.9896	0.9734

### 3.3.3. L–F isotherm

The L–F isotherm model is essentially a Freundlich isotherm that approaches an adsorption maximum at high concentration of adsorbate. The L–F equation can also be mathematically obtained by assuming that the surface is homogeneous, but that the adsorption is a cooperative process due to adsorbate–adsorbate interactions [4]. The following Eq. (10) represents this model:

$$q_e = \frac{Q^0 b C_e^{\frac{1}{n}}}{1 + b C_e^{\frac{1}{n}}} \quad (10)$$

The parameters of L–F model (shown in Table 1) were obtained by non-linear curve fitting using Levenberg–Marquardt algorithm. The correlation coefficient  $R^2$  above 0.9734 at the selected temperature, and both  $b$  and  $n$  increased with the increasing temperature, which was consistent with the variation of  $Q^0$  indicating endothermic nature of the adsorption. The results show that adsorption of RBB onto okara can be well described by L–F isotherm model (Fig. 7(c)).

Reported  $Q^0$  values of other low-cost adsorbents for the adsorption of reactive dyes were listed in Table 2.  $Q^0$  in this study was 68.67 mg/g, which was comparable to those of some other adsorbents, clearly indicating that okara was an efficient and low-cost adsorbent for the removal of reactive dyes from wastewater.

### 3.4. Adsorption kinetics

In order to design an efficient and effective model for the adsorption processes of RBB onto okara, the evaluation of kinetic parameters is essential. Three kinetic models have been widely used in the literature for adsorption processes: (i) pseudo-first-order kinetic model (Lagergren model) [44]; (ii) pseudo-second-order kinetic model (Ho and McKay model) [45]; (iii) intra-particle diffusion kinetic model (Webber and Morris model) [46].

#### 3.4.1. Pseudo-first-order kinetic model

The Eq. (11) given below represents Lagergren's pseudo-first-order rate equation [44]:

$$\log(q_e - q_t) = \log q_e - \frac{k_1 t}{2.303} \quad (11)$$

where  $q_t$  is the dye amounts adsorbed per unit mass of adsorbent at time  $t$  (mg/g) and  $k_1$  is the pseudo-first-order rate constant for the adsorption process ( $\text{min}^{-1}$ ). The Fig. 8(a) was plotted between  $\log(q_e - q_t)$  versus time, the slope of which gives the value of  $k_1$ .

In most cases, it has been reported that the adsorption data were well represented by the Lagergren first-order kinetic model, but only in the first 30–50 min of the adsorption process. The values of  $k_1$  and  $q_e$  were listed in Table 3. For pseudo-first-order kinetic model, the values of  $R^2$  were found to be 0.9719–0.9927, but the theoretical values  $q_{e,\text{cal}}$  were much lower than the experimental values  $q_{e,\text{exp}}$  at different initial concentrations. These results indicate that

Table 2  
Adsorption capacity for the removal of reactive dyes from aqueous solutions by some low-cost adsorbents

Adsorbent	Dye	$Q^0$ (mg/g)	Reference
Modified basic oxygen furnace slag	RBB	60	[32]
Cross-linked chitosan/oil palm ash composite beads	RBB	416.7	[36]
Wheat bran	RBB	97.1	[37]
Waste metal hydroxide sludge	RBB	275	[38]
<i>Pinus sylvestris</i> Linneo	Reactive red 195	6.69	[39]
Sepia pen	Reactive Green 12	3.46	[40]
High lime soma fly ash	Reactive Black 5	7.184	[41]
Barley straw	Reactive Black 5	25.4	[42]
Fly ash	RBB	135.69	[43]
Okara	RBB	68.7	This study

the pseudo-first-order model was not appropriate to describe the adsorption process of RBB onto okara.

### 3.4.2. Pseudo-second-order kinetic model

The pseudo-second-order kinetic model was applied for the interpretation of experimental data. The pseudo-second-order kinetic model of Ho and McKay [45] is represented as Eq. (12):

$$\frac{1}{q_t} = \frac{1}{k_2 q_e^2} + \frac{1}{q_e} t \quad (12)$$

where  $k_2$  is the pseudo-second order rate constant for the adsorption process (g/(mg min)). By plotting of  $t/q_t$  versus  $t$  for different initial RBB concentrations, linear lines were obtained as shown in Fig. 8(b). The constants calculated from slope and intercept of linear lines were given in Table 3. The correlation coefficients  $R^2$  for the pseudo-second-order kinetic plots were found to be equal to 1 and the theoretical values  $q_{e,cal}$  agreed well with the experimental values  $q_{e,exp}$ . The rate constant  $k_2$  decreased from 0.1550 to 0.0781 g/(mg·min) with the increasing RBB concentrations (Table 3). Hence, it was proved that the adsorption process of RBB onto okara was a pseudo-second-order reaction.

### 3.4.3. Intra-particle diffusion kinetic model

The adsorption of dye onto a solid phase material is a multi-step process and it is assumed that four steps are involved: bulk diffusion, boundary layer diffusion, intra-particle diffusion, and physical and/or chemical adsorption reaction. It has been reported from numerous studies that bulk diffusion can be negligible if a sufficient stirring speed is used [47]. This study was carried out under the condition that the stirring speed was 150 rpm, so the first step could not be rate-limited. The fourth step was considered to be an equilibrium reaction that was assumed to be negligible in terms of rapid reaction speed in the study. Thus, the dye adsorption rate was limited usually by either boundary layer diffusion or intra-particle diffusion. So the experimental data were analyzed using the intra-particle diffusion model proposed by Weber and Morris [46], written as Eq. (13):

$$q_t = k_{int} t^{0.5} + I \quad (13)$$

where  $k_{int}$  is the intra-particle diffusion rate constant (mg/(g·min<sup>1/2</sup>)) determined from the slope and  $I$  is

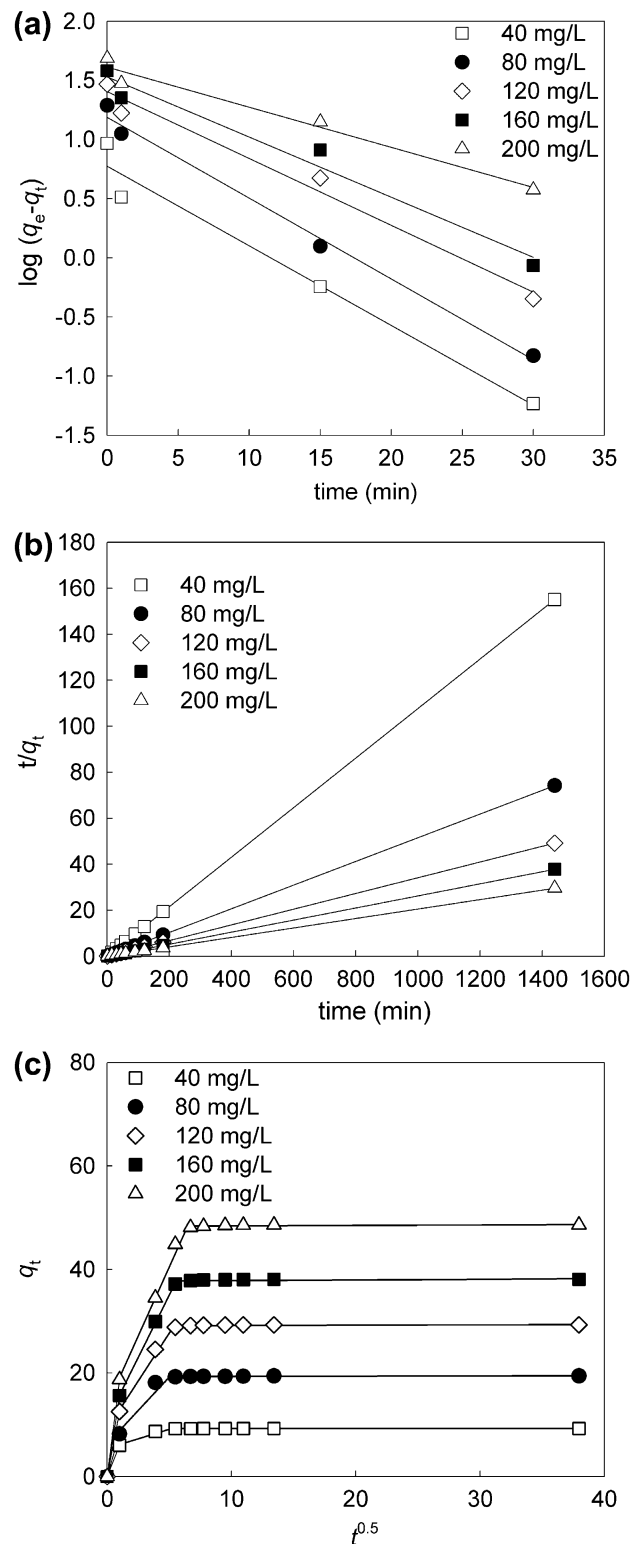


Fig. 8. Kinetic models for adsorption of RBB by okara at different initial concentrations. (a) Pseudo-first-order model; (b) pseudo-second-order model; (c) intra-particle diffusion model ( $C_0 = 40, 80, 120, 160,$  and  $200$  mg/L, temperature =  $20 \pm 1^\circ\text{C}$ , adsorbent dosage =  $4$  g/L, initial pH value  $2.0 \pm 0.1$ ).

Table 3  
Kinetic parameters of RBB adsorbed onto okara at different initial concentrations

$C_0$ (mg/L)	Pseudo-first-order kinetic model			Pseudo-second-order kinetic model			
	$R^2$	$k_1$ ( $\text{min}^{-1}$ )	$q_{e,\text{cal}}$ (mg/g)	$R^2$	$k_2$ (g/(mg min))	$q_{e,\text{cal}}$ (mg/g)	$q_{e,\text{exp}}$ (mg/g)
40	0.9729	0.1550	2.17	1	0.3648	9.29	9.28
80	0.9927	0.1573	3.28	1	0.1005	19.42	19.40
120	0.9813	0.1301	4.08	1	0.0482	29.33	29.30
160	0.9719	0.1172	4.62	1	0.0278	38.17	38.08
200	0.9735	0.0781	5.01	1	0.0133	48.78	48.61
Intra-particle diffusion							
	$R^2$	$k_{\text{int}}$ (mg/(g min <sup>1/2</sup> ))		$I$ (mg/g)			
40	0.9558	0.7401		5.4320			
80	0.9285	2.5824		6.2952			
120	0.9890	3.7046		9.2062			
160	0.9995	4.8332		10.9240			
200	0.9893	5.3357		13.7980			

the intercept (mg/g) which is proportional to the thickness of the boundary layer. As shown in Fig. 8(c), all the curves had the same features: an initial curve portion was followed by a linear portion and then a plateau, indicating that there were different stages in the adsorption process of RBB onto okara. The initial portion was possibly due to boundary layer diffusion, the second linear portion to the intra-particle diffusion, and the final plateau to the equilibrium. If intra-particle diffusion would be the only rate-limiting step, the second linear line should pass through the origin, indicating the first step did not exist. However, in the present study, the second linear line did not pass through the origin, which expressed that the intra-particle diffusion was not the only rate-limiting step and boundary layer diffusion might be involved in the adsorption. The values of  $k_{\text{int}}$  and  $I$  obtained from the second linear portion were listed in Table 3. The  $k_{\text{int}}$  was higher at a higher initial RBB concentration, suggesting the increasing influence of dye concentration gradient. Values of  $I$  increased with the increase of initial RBB concentration. As shown in Fig. 8(c), the  $k_{\text{int}}$  increased with the increasing  $I$  values, supporting the idea that the larger the intercept the greater the boundary layer effect. The values of correlation coefficients  $R^2$  for second section were within the range of 0.9285 and 0.9995, suggesting that intra-particle diffusion model well fitted the experimental data. Similar observation was also reported for the biosorption of Acid Yellow 17 onto non-living aerobic granules [1].

### 3.5. Thermodynamic analysis

In order to evaluate the thermodynamic parameters for adsorption of RBB onto okara, the adsorption

studies were carried out at different temperatures 20, 35, and 50°C. The Gibbs free energy change ( $\Delta G^\circ$ ) of the adsorption can be calculated according to Eqs. (14) and (15):

$$\Delta G^\circ = -RT \ln K_p \quad (14)$$

$$K_p = \frac{C_0 - C_e}{C_e} \quad (15)$$

where  $R$  is the gas constant;  $T$  is the temperature in K;  $K_p$  is the equilibrium constant. The enthalpy change ( $\Delta H^\circ$ ) and entropy change ( $\Delta S^\circ$ ) are obtained from Van't Hoff (Eq. (16)):

$$\ln K_p = \frac{\Delta S^\circ}{R} - \frac{\Delta H^\circ}{RT} \quad (16)$$

When the temperature increased from 20 to 35 and 50°C,  $\Delta G^\circ$  decreased from  $-7.40$  to  $-8.53$  and  $-9.85$  kJ/mol, indicating that the reactions were spontaneous because of the negative  $\Delta G^\circ$ , and the adsorption was more favorable at high temperature. The values of  $\Delta H^\circ$  and  $\Delta S^\circ$  obtained from the slope and intercept of the plot of  $\ln(K_p)$  vs.  $1/T$  (Figures are not shown here,  $R^2 = 0.9948$ ). The positive values of  $\Delta H^\circ$  (26.33 kJ/mol) accounted for the endothermic nature, while positive  $\Delta S^\circ$  values (114.93 J/(mol·K)) reflected the affinity of the adsorbate toward adsorbent [48].

## 4. Conclusions

The adsorption of RBB from aqueous solution onto okara has been studied. The adsorption process was

highly dependent on the acidic pH and the favorable pH value was 2.0. Okara was abundant in many parts of the world, and could serve as a cheap and easily available source for the production of adsorbents. L–F isotherm was applicable for describing the equilibrium data, and  $Q^0$  was 68.67, 159.60, and 402.58 mg/g at 20, 35, and 50°C, respectively. The pseudo-second-order model expressed the adsorption kinetics well. Intra-particle diffusion model indicated that both boundary layer and intra-particle diffusion might affect the adsorption rate. Thermodynamic studies indicated that the adsorption process was spontaneous and endothermic. The FTIR analysis revealed that functional groups (e.g. amine, hydroxyl, and carboxyl) on okara would be the active binding sites. The study demonstrated that okara could be applied as a kind of cheap, novel, alternative, and effective adsorbent to remove RBB from wastewater.

### Acknowledgements

The authors wish to thank the NSFC (51078007, 51378027), BJ-NSF (8112007), PHR-IHLB (PHR201-10819), and Beijing Talent Foundation of BJUT (2013-JH-L06) for the financial supports of this study.

### References

- [1] J.F. Gao, Q. Zhang, K. Su, R.N. Chen, Y.Z. Peng, Biosorption of Acid Yellow 17 from aqueous solution by non-living aerobic granular sludge, *J. Hazard. Mater.* 174 (2010) 215–225.
- [2] J.F. Gao, Q. Zhang, J.H. Wang, X.L. Wu, S.Y. Wang, Y.Z. Peng, Contributions of functional groups and extracellular polymeric substances on the biosorption of dyes by aerobic granules, *Biores. Technol.* 102 (2011) 805–813.
- [3] S. Papić, D. Vujević, N. Koprivanac, D. Šinko, Decolorization and mineralization of commercial reactive dyes by using homogeneous and heterogeneous Fenton and UV/Fenton processes, *J. Hazard. Mater.* 164 (2009) 1137–1145.
- [4] Z. Aksu, Application of biosorption for the removal of organic pollutants: A review, *Process Biochem.* 40 (2005) 997–1026.
- [5] T. Robinson, G. McMullan, R. Marchant, P. Nigam, Remediation of dyes in textile effluent: A critical review on current treatment technologies with a proposed alternative, *Biores. Technol.* 77 (2001) 247–255.
- [6] Q. Zhuo, H. Ma, B. Wang, L. Gu, Catalytic decolorization of azo-stuff with electro-coagulation method assisted by cobalt phosphomolybdate modified kaolin, *J. Hazard. Mater.* 142 (2007) 81–87.
- [7] I. Oller, S. Malato, J.A. Sánchez-Pérez, Combination of advanced oxidation processes and biological treatments for wastewater decontamination—A review, *Sci. Total Environ.* 409 (2011) 4141–4166.
- [8] S. Rodríguez Couto, Dye removal by immobilised fungi, *Biotechnol. Adv.* 27 (2009) 227–235.
- [9] M.E. Russo, F. Di Natale, V. Prigione, V. Tigini, A. Marzocchella, G.C. Varese, Adsorption of acid dyes on fungal biomass: Equilibrium and kinetics characterization, *Chem. Eng. J.* 162 (2010) 537–545.
- [10] J. Mittal, D. Jhare, H. Vardhan, A. Mittal, Utilization of bottom ash as a low-cost sorbent for the removal and recovery of a toxic halogen containing dye Eosin Yellow, *Desalin. Water Treat.* (2013) 1–12.
- [11] A. Mittal, L. Kurup, Column operations for the removal and recovery of a hazardous dye ‘Acid Red-27’ from aqueous solutions, using waste materials—Bottom ash and de-oiled soya, *Ecol. Environ. Conserv.* 12 (2006) 181–186.
- [12] V.K. Gupta, A. Mittal, D. Jhare, J. Mittal, Batch and bulk removal of hazardous colouring agent Rose Bengal by adsorption techniques using bottom ash as adsorbent, *RSC Adv.* 2 (2012) 8381–8389.
- [13] J. Mittal, V. Thakur, A. Mittal, Batch removal of hazardous azo dye Bismark Brown R using waste material hen feather, *Ecol. Eng.* 60 (2013) 249–253.
- [14] A. Mittal, D. Jhare, J. Mittal, Adsorption of hazardous dye Eosin Yellow from aqueous solution onto waste material de-oiled soya: Isotherm, kinetics and bulk removal, *J. Mol. Liq.* 179 (2013) 133–140.
- [15] A. Mittal, V. Thakur, V. Gajbe, Adsorptive removal of toxic azo dye Amido Black 10B by hen feather, *Environ. Sci. Pollut. R.* 20 (2013) 260–269.
- [16] A. Mittal, V. Thakur, J. Mittal, H. Vardhan, Process development for the removal of hazardous anionic azo dye Congo Red from wastewater by using hen feather as potential adsorbent, *Desalin. Water Treat.* (2013) 1–11, doi: [10.1080/19443994.2013.785030](https://doi.org/10.1080/19443994.2013.785030).
- [17] A. Mittal, Removal of the dye, Amaranth from waste water using hen feathers as potential adsorbent, *Electron. J. Environ. Agric. Food Chem.* 5 (2006) 1296–1305.
- [18] A. Mittal, J. Mittal, L. Kurup, Utilization of hen feathers for the adsorption of Indigo Carmine from simulated effluents, *J. Environ. Prot. Sci.* 1 (2007) 92–100.
- [19] A. Mittal, R. Jain, J. Mittal, S. Meenakshi, Adsorptive removal of hazardous dye Quinoline Yellow from wastewater using coconut-husk as potential adsorbent, *Fresenius Environ. Bull.* 19 (2010) 1171–1179.
- [20] A. Mittal, R. Jain, J. Mittal, S. Varshney, S. Sikarwar, Removal of Yellow ME 7 GL from industrial effluent using electrochemical and adsorption techniques, *Int. J. Environ. Pollut.* 43 (2010) 308–323.
- [21] H. Daraei, A. Mittal, M. Noorisepehr, F. Daraei, Kinetic and equilibrium studies of adsorptive removal of phenol onto eggshell waste, *Environ. Sci. Pollut. R.* 20 (2013) 4603–4611.
- [22] H. Daraei, A. Mittal, J. Mittal, H. Kamali, Optimization of Cr(VI) removal onto biosorbent eggshell membrane: Experimental & theoretical approaches, *Desalin. Water Treat.* (2013) 1–9, doi: [10.1080/19443994.2013.787374](https://doi.org/10.1080/19443994.2013.787374).
- [23] H. Daraei, A. Mittal, M. Noorisepehr, J. Mittal, Separation of chromium from water samples using eggshell powder as a low-cost sorbent: Kinetic and thermodynamic studies, *Desalin. Water Treat.* (2013) 1–7, doi: [10.1080/19443994.2013.837011](https://doi.org/10.1080/19443994.2013.837011).

- [24] M.R. Kosseva, Processing of food wastes, in: S.L. Taylor (Ed.), *Advances in Food and Nutrition Research*, Academic Press, San Diego, CA, 2009 (Chapter 3), pp. 57–136.
- [25] D.K. O'Toole, Characteristics and use of okara, the soybean residue from soy milk production: A review, *J. Agric. Food Chem.* 47 (1999) 363–371.
- [26] B. Li, M. Qiao, F. Lu, Composition, nutrition, and utilization of okara (soybean residue), *Food Rev. Int.* 28 (2011) 231–252.
- [27] E.J. Weber, V.C. Stickney, Hydrolysis kinetics of reactive blue 19-vinyl sulfone, *Water Res.* 27 (1993) 63–67.
- [28] V.K. Gupta, Suhas, application of low-cost adsorbents for dye removal—A review, *J. Environ. Manage.* 90 (2009) 2313–2342.
- [29] A.B. dos Santos, I.A.E. Bisschops, F.J. Cervantes, J.B. Van Lier, The transformation and toxicity of anthraquinone dyes during thermophilic (55°C) and mesophilic (30°C) anaerobic treatments, *J. Biotechnol.* 115 (2005) 345–353.
- [30] Y. Lu, Y. Tan, Research on toxic effects of *Saccharomyces Cerevisiae* by reactive brilliant blue KN-R, *Guangzhou Chem. Ind. (in Chinese)* 39 (2011) 97–98.
- [31] A. Mittal, J. Mittal, L. Kurup, Adsorption isotherms, kinetics and column operations for the removal of hazardous dye, Tartrazine from aqueous solutions using waste materials—Bottom ash and de-oiled soya, as adsorbents, *J. Hazard. Mater.* 136 (2006) 567–578.
- [32] Y. Xue, H. Hou, S. Zhu, Adsorption removal of reactive dyes from aqueous solution by modified basic oxygen furnace slag: Isotherm and kinetic study, *Chem. Eng. J.* 147 (2009) 272–279.
- [33] Ö. Gök, A.S. Özcan, A. Özcan, Adsorption behavior of a textile dye of Reactive Blue 19 from aqueous solutions onto modified bentonite, *Appl. Surf. Sci.* 256 (2010) 5439–5443.
- [34] I. Langmuir, The adsorption of gases on plane surfaces of glass, mica and platinum, *J. Am. Chem. Soc.* 40 (1918) 1361–1403.
- [35] H. Freundlich, Ueber die adsorption in loesungen, *Z. Phys. Chem.* 57 (1907) 385–470.
- [36] M. Hasan, A.L. Ahmad, B.H. Hameed, Adsorption of reactive dye onto cross-linked chitosan/oil palm ash composite beads, *Chem. Eng. J.* 136 (2008) 164–172.
- [37] F. Çiçek, D. Özer, A. Özer, A. Özer, Low cost removal of reactive dyes using wheat bran, *J. Hazard. Mater.* 146 (2007) 408–416.
- [38] S.C.R. Santos, V.J.P. Vilar, R.A.R. Boaventura, Waste metal hydroxide sludge as adsorbent for a reactive dye, *J. Hazard. Mater.* 153 (2008) 999–1008.
- [39] O. Aksakal, H. Uzun, Equilibrium, kinetic and thermodynamic studies of the biosorption of textile dye (Reactive Red 195) onto *Pinus sylvestris* L, *J. Hazard. Mater.* 181 (2010) 666–672.
- [40] S.A. Figueiredo, R.A. Boaventura, J.M. Loureiro, Color removal with natural adsorbents: Modeling, simulation and experimental, *Sep. Purif. Technol.* 20 (2000) 129–141.
- [41] Z. Eren, F.N. Acar, Equilibrium and kinetic mechanism for Reactive Black 5 sorption onto high lime Soma fly ash, *J. Hazard. Mater.* 143 (2007) 226–232.
- [42] B.C. Oei, S. Ibrahim, S. Wang, H.M. Ang, Surfactant modified barley straw for removal of acid and reactive dyes from aqueous solution, *Biores. Technol.* 100 (2009) 4292–4295.
- [43] N. Dizge, C. Aydinler, E. Demirbas, M. Kobya, S. Kara, Adsorption of reactive dyes from aqueous solutions by fly ash: Kinetic and equilibrium studies, *J. Hazard. Mater.* 150 (2008) 737–746.
- [44] S. Lagergren, Zur theorie der sogenannten adsorption gelöster stoffe, *K. Sven. Vetenskapsakad. Handl.* 24 (1898) 1–39.
- [45] Y.S. Ho, G. McKay, Pseudo-second order model for sorption processes, *Process Biochem.* 34 (1999) 451–465.
- [46] W.J. Weber, J.C. Morris, Kinetics of adsorption on carbon from solution, *J. Sanit. Eng. Div., ASCE* 89 (1963) 31–59.
- [47] G. Crini, P.M. Badot, Application of chitosan, a natural aminopolysaccharide, for dye removal from aqueous solutions by adsorption processes using batch studies: A review of recent literature, *Prog. Polym. Sci.* 33 (2008) 399–447.
- [48] R. Niwas, U. Gupta, A.A. Khan, K.G. Varshney, The adsorption of phosphamidon on the surface of styrene supported zirconium (IV) tungstophosphate: A thermodynamic study, *Colloid Surf. A* 164 (2000) 115–119.